Available online at www.sciencedirect.com
ScienceDirect
Trans. Nonferrous Met. Soc. China 31(2021) 2762−2772
Transactions of Nonferrous Metals Society of China
www.tnmsc.cn

Fracture pattern evolution of SnAgCu−SnPb mixed solder joints at cryogenic temperature

Ming WU, Shan-lin WANG, Wen-jun SUN, Min HONG, Yu-hua CHEN, Li-ming KE

Jiangxi Key Laboratory of Forming and Joining Technology for Aerospace Components, Nanchang Hangkong University, Nanchang 330063, China

Received 6 September 2020; accepted 28 June 2021

Abstract: The effect of cryogenic temperatures on the mechanical properties and fracture mechanism of SnAgCu−SnPb mixed solder joints was investigated. The results showed that the tensile strength of mixed solder joints first increased with the increase of Pb content and reached its maximum at 22.46 wt.% Pb; subsequently, it decreased as Pb content increased. However, cryogenic temperatures improved the tensile strength of the solder joints. Both Pb content and cryogenic temperature caused the fracture mode of the mixed solder joints to change; however, temperature remained the main influencing factor. As the temperature fell from 298 to 123 K, the failure pattern in the solder joints transformed from ductile fracture to quasi-ductile fracture to quasi-brittle fracture and finally, to brittle fracture.
Key words: fracture pattern; tensile strength; SnAgCu−SnPb solder; cryogenic temperature

1 Introduction

In the past few decades, Sn−37Pb eutectic solder has been widely used owing to its excellent properties and low cost. However, Pb has an adverse effect on the environment and human health because of its toxicity [1]. Because EU legislation restricts the use of Pb solder, lead-free solders, especially Sn3.0Ag0.5Cu (SAC305) solder alloys [2], have become popular. In lead-free solder alloy processing, Pb pollution is inevitable due to recycling and mixed assembly [3]. In addition, Sn−Pb solders are still used in critical applications (aerospace, military, etc.) to ensure product reliability. Pb pollution may also occur during repair processes because of legal stipulations and several other reasons [4]. In aerospace applications, the exposed electronic components are subjected to extreme temperatures due to the huge temperature gradients that exist in space and on the surface of different heavenly bodies, for instance, under the condition of Moon (77−423 K), Mars (133−293 K) and Giant Planets (133−653 K) [5−7]. As they are used to link electronic components, solder joints play an important role in mechanical connection, electrical control and signal channels. Their performance and quality have an important influence on the overall function of the electronic components [8−10].

Temperature is critical to the mechanical properties and fracture of the solder joints. Till date, several scholars have studied the microstructure, thermodynamics, and mechanical properties in the temperature range of 218−423 K [11,12]. However, there are few reports on the mechanical properties of solder joints at cryogenic temperatures (below 218 K). TIAN et al [6] studied the fracture mode of SAC305 solder joints at 77−298 K and found that the reduction in temperature would cause the failure mode of the solder joints to transition from ductile to brittle fracture. FINK et al [13] and YAO

Corresponding author: Shan-lin WANG, Tel: +86-13755603426, E-mail: slwang70518@nchu.edu.cn
DOI: 10.1016/S1003-6326(21)65691-1

et al [14] found that, as the temperature decreases, the tensile strength of the solder joint does not increase or decrease monotonically, but rather, first increases and then decreases. Based on several studies, three basic failure modes have been identified for solder joints in the temperature range of 218−473 K, namely, ductile failure inside the solder, brittle failure of the IMC layer, and mixed ductile–brittle fracture between the two [15−17]. However, some scholars have found that the solder joints fractured inside the solder at 166 K, but the fracture mode was brittle [18]. From the above studies, the fracture mechanism of solder joints, especially mixed solder joints at low temperatures, has not been explored much and the results are often controversial.

In this study, Sn−37Pb solder alloys were mixed with SAC305 solder alloys to make mixed solder with different Pb contents, and the Cu/Solder/Cu joints were tested at cryogenic temperatures to evaluate their mechanical properties. The fracture location and mechanism are determined by analyzing the fracture surface. In addition, the effect of Pb content and different cryogenic temperatures on the fracture mode and tensile properties of the solder joints were investigated to provide experimental data and theoretical references for the failure of mixed solder joints at cryogenic temperatures.

2 Experimental

In this study, mixed solders with different contents of Pb (0, 4.67, 22.46, 37 wt.%) were fabricated by adding Sn−37Pb solder alloys to SAC305 solder alloys (Table 1). A certain proportion of the mixed solders were placed in a crucible, and 5 wt.% $ZnCl_2$ rosin flux was dripped into it. The crucible was placed in a reflow soldering machine (TYR108C) for 81s at 503 K. The uniform composition of the mixed solders was ensured by repetitive smelting three times. After the smelting was completed, X-ray equipment (X7600NT, DAGE) was used to select defect-free solder balls having the same size, which were placed in anhydrous alcohol and cleaned ultrasonically (KH−50B, Hechuang) for 5 min. The volume of the mixed solder balls was (0.070±0.0025) mm^3 and the diameter was (500±5) μm.

The printed circuit board (PCB) of Cu pads with a diameter of 420 μm and thickness of 37 μm was processed by organic solderability preservatives (OSP). The solder joints had a Cu/Solder/Cu sandwich structure prepared by the double plate lap method. The prepared solder joint specimens were placed into the reflow machine, where the peak temperature was 533 K and the holding time above the liquid phase line was 60 s. Figure 1 shows the microstructure of solder joints

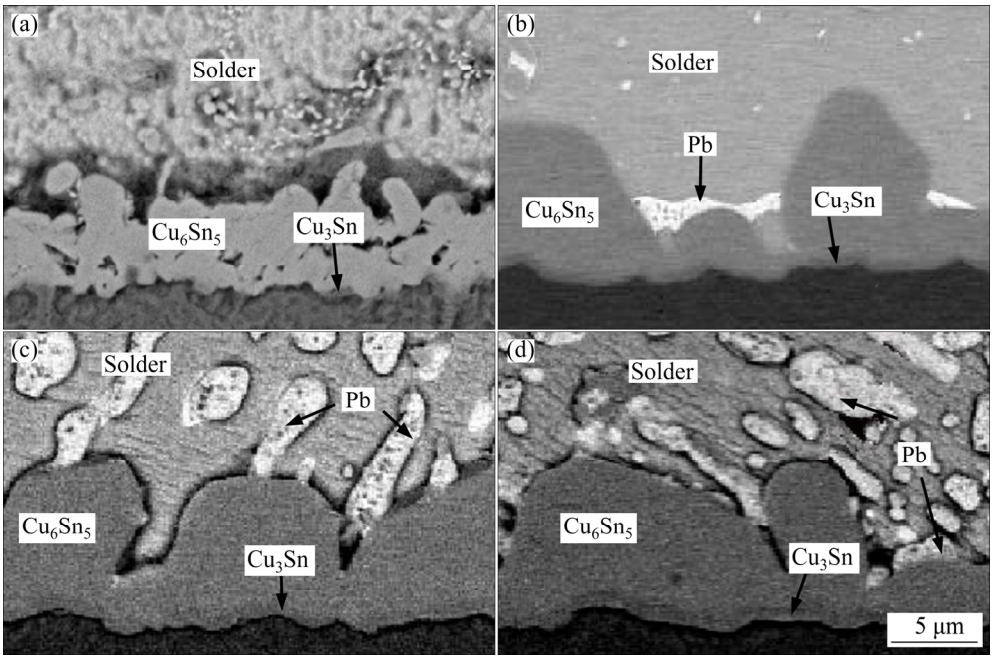

Fig. 1 Microstructures of solder joints with different Pb contents: (a) 0 wt.%; (b) 4.67 wt.%; (c) 22.46 wt.%; (d) 37 wt.%

with different Pb contents, which is mainly composed of solder body and intermetallic compound (IMC) layers. Then, the solder joints were tested using a thermal-mechanical dynamic analyzer (TQ800, TA) that could deliver atomized liquid nitrogen to the chamber where the sample was located and attain the required temperature (298, 223, 173, 123 K) for this experiment by adjusting the degree of atomization of liquid nitrogen. Subsequently, the sample was mounted on a tensile fixture and the shear rate was set to be 50 μm/min as shown in Fig. 2. Three samples were tested corresponding to each test condition, and the fracture surface of the tensile samples was examined with a scanning electron microscope (SEM, Hitachi, S−2500) equipped with an energy dispersive spectrometer (EDS).

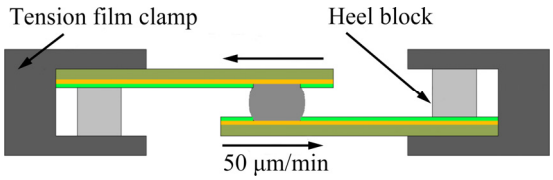

Fig. 2 Schematic diagram of solder joint stretching

3 Results

3.1 Tensile strength

The stress−strain curve and tensile strength of SAC305 solder joints at different temperatures are shown in Fig. 3. It can be seen from Fig. 3(a) that the decrease in temperature had a great influence on the tensile process of the solder joints. The typical stages in the tensile process of the solder joints were those of elastic deformation and plastic deformation, followed by the final fracture. The solder had an obvious region of gentle plasticity and yielded at 298 K. After reaching the highest strength, the curve slowly decreased to the point corresponding to the lowest stress, showing strong ductile fracture properties. With the decrease in temperature to 223 K and subsequently, 173 K, the deformation rate of the solder decreased and the slope of the elastic-plastic zone increased, which indicated that the hardening rate of the solder joint increased with the decrease in temperature. When the temperature continued to drop to 123 K, the curve became a smooth line and failure occurred without yielding, indicating that the failure mode of the solder joint at this time are brittle fracture. From Fig. 3(b), the tensile strength increased as the temperature decreased. Further, the lower the temperature, the higher the growth rate.

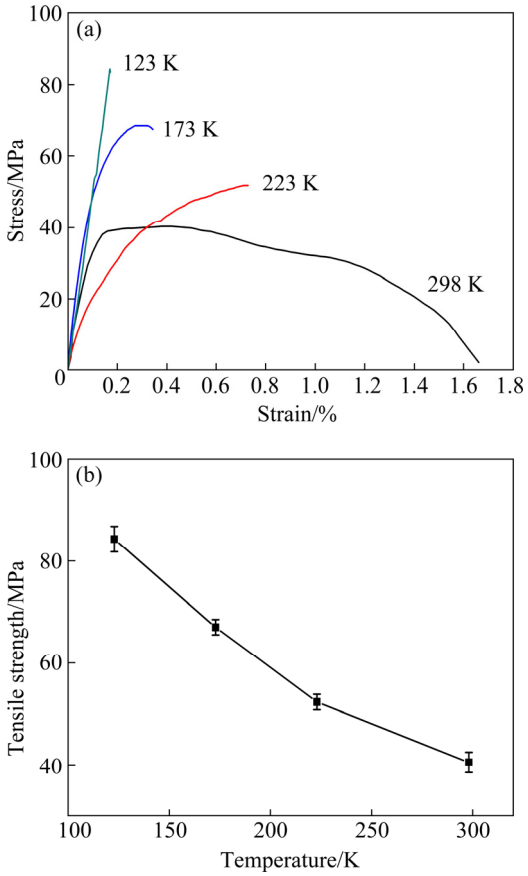

Fig. 3 Stress−strain curves (a) and tensile strength (b) of SAC305 solder joints at different temperatures

Figure 4 shows the trend of the stress−strain curves of the mixed solder joints with temperature. Like SAC305 solder joints, the toughness characteristics of the solder continued to weaken with decreasing temperature. The slope gradient of the stress−strain curve suddenly became steep at 123 K, which meant that the solder joint fractured instantaneously at 123 K. Figure 4(d) shows the tensile strength of solder joints at different temperatures and Pb contents. The tensile strength of the solder was comparable to that of the SAC305 joint (Fig. 3(b)) and showed an upward trend. It is worth noting that with the increase in Pb content, the tensile strength reached the highest level at 22.46 wt.% and then decreased. However, compared with the solder having low Pb content (4.67 wt.%), the solder with high Pb content (37 wt.%) had better tensile properties, and the performance was the best when the Pb content was 22.46 wt.%.

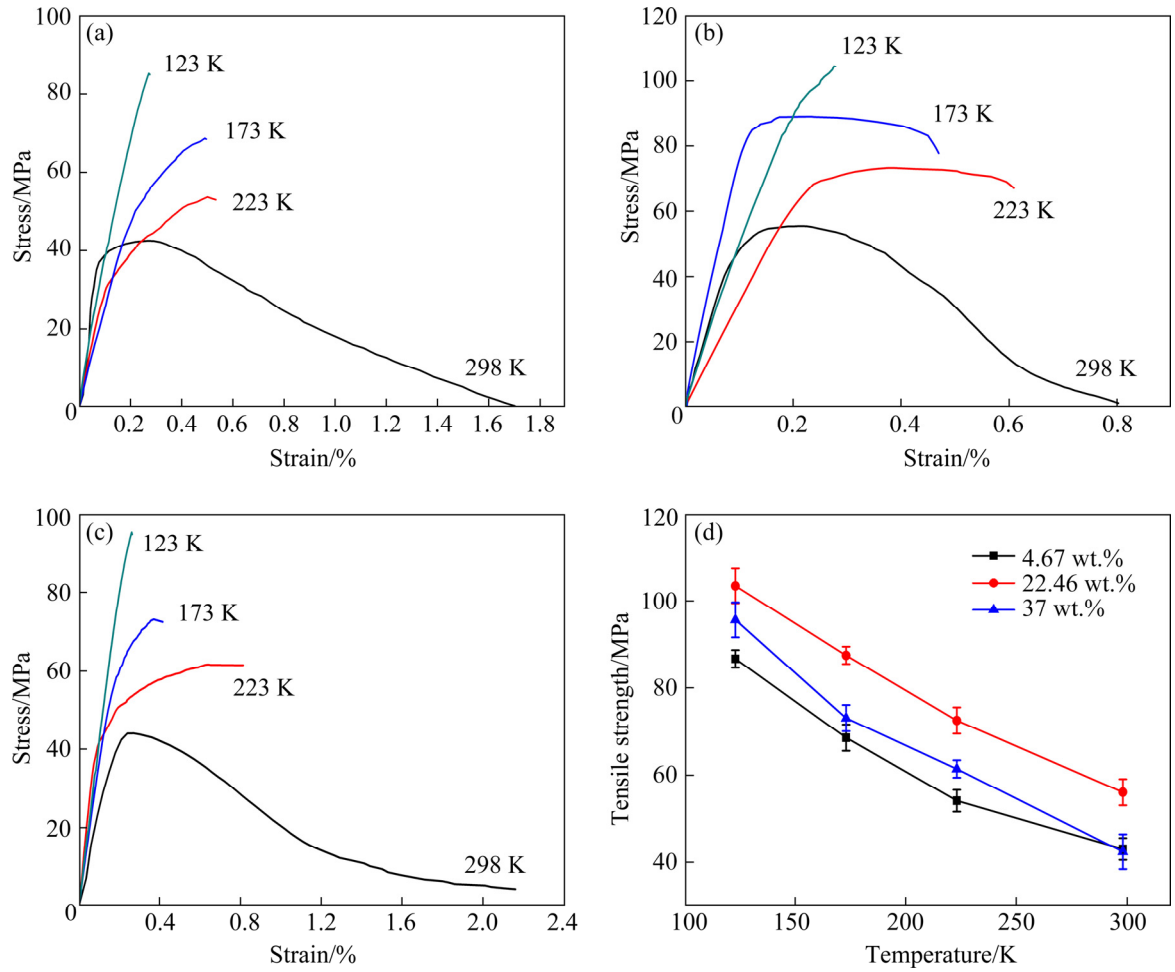

Fig. 4 Stress−strain curves (a−c), and tensile strength diagram (d) of mixed solder joints at different temperatures and Pb contents: (a) 4.67 wt.%; (b) 22.46 wt.%; (c) 37 wt.%

3.2 Fracture morphology

To further study the effect of different temperatures and Pb contents on the transition of the fracture mechanism of solder joints, it is necessary to analyze the fracture surface. Figure 5 shows the fracture morphology of SAC305 solder joints at normal as well as cryogenic temperatures. Figures 5(a, b) showed that there were obvious dimples and tearing edges on the fracture surface. The facets of the tearing unit were surrounded by the tearing ridges. They were connected by zones of plastic deformation, and there were holes in the middle of the solder joints. These phenomena indicated that the fracture mode was ductile at 298 and 223 K. In contrast, the fracture surface distribution was more complex at 173 K. The mixture of solder and IMC showed mixed transgranular and intergranular fracture and there were many cracks. With the further decrease in temperature (Fig. 5(d)), the fracture surface was completely transferred to the IMC layer, indicating that there was massive clastic Cu_6Sn_5 distribution on the fracture surface. As brittle materials, Cu_6Sn_5 and Cu_3Sn IMCs indicated that the brittle fracture of solder occurred at 123 K, which was consistent with the conclusions of the stress−strain curve analysis in Fig. 3. It is worth noting that the cracks in the solder at 123 K were different from the tiny cracks at 173 K, and it penetrated the entire IMC layer, resulting in potentially catastrophic damage.

The fracture surface of the mixed solder joints with 4.67 wt.% and 22.46 wt.% Pb at different temperatures are shown in Figs. 6 and 7. It can be clearly seen from Figs. 6(a, b) that the joint broke inside the solder at 298 and 223 K, which meant that the fracture mode was ductile. As the temperature decreased, the fracture position was transferred to the junction of the solder and the IMC layer, and the flower-like solder on the fracture

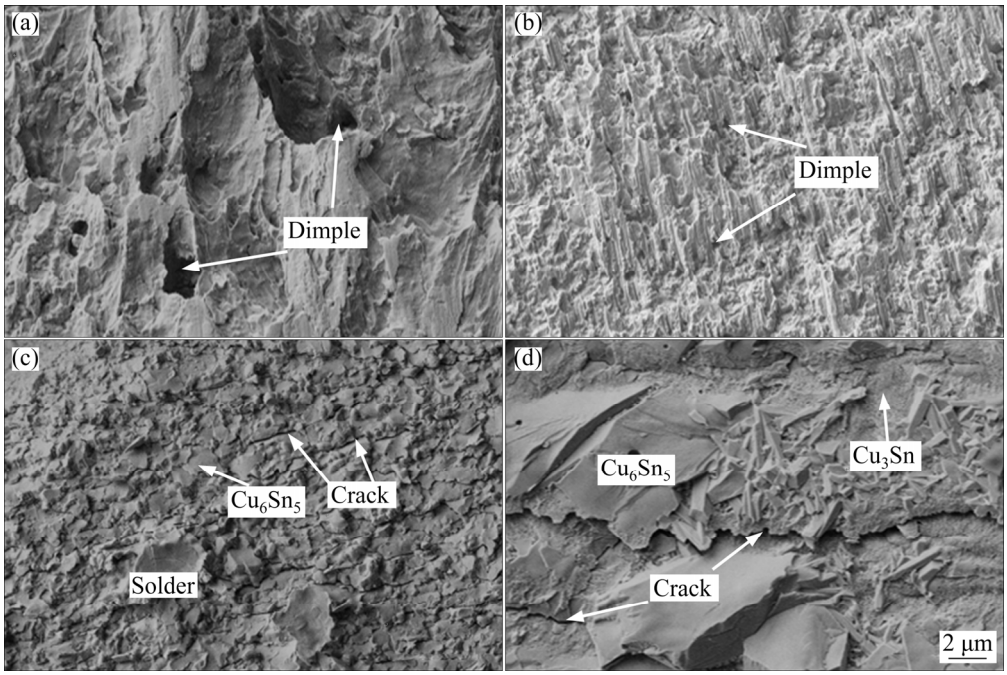

Fig. 5 Fracture surface morphology of SAC305 solder joints at different temperatures: (a) 298 K; (b) 223 K; (c) 173 K; (d) 123 K

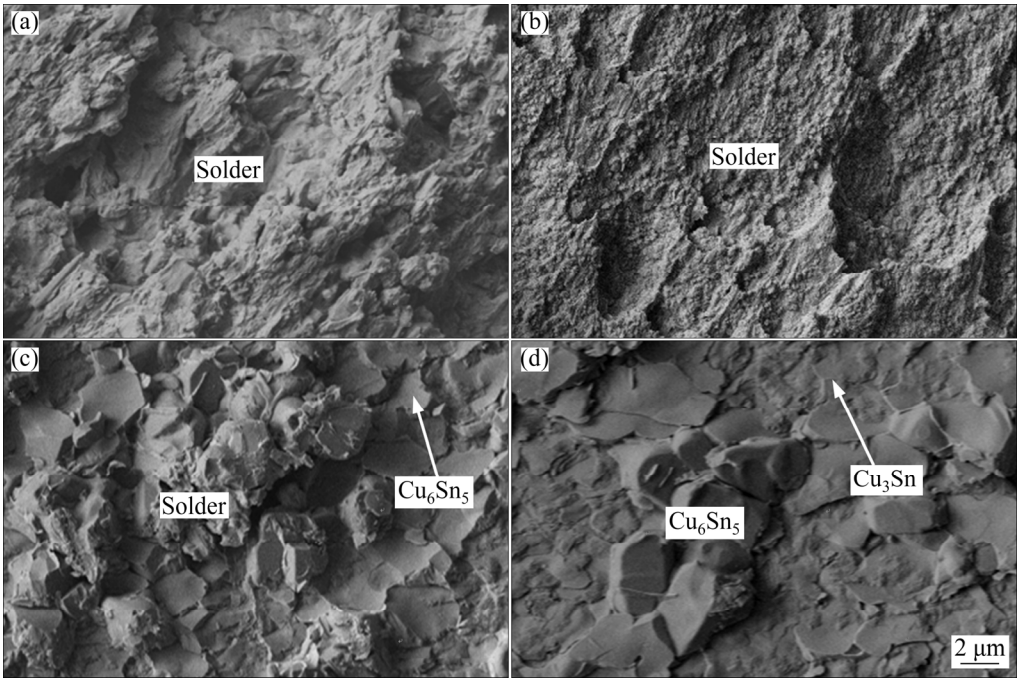

Fig. 6 Fracture surface morphology of mixed solder joints with 4.67 wt.% Pb at different temperatures: (a) 298 K; (b) 223 K; (c) 173 K; (d) 123 K

surface was mixed with bulk IMC (Fig. 6(c)). As the temperature dropped to 123 K, the fracture surface was transferred to the IMC layer and located between Cu_6Sn_5 and Cu_3Sn (Fig. 6(d)). When the Pb content increased to 22.46 wt.% (Fig. 7), the fracture morphology of mixed solder joint produced at 298 and 223 K (Figs. 7(a, b)) resembled that of the 4.67 wt.% Pb. However, the mixture that adhered to the IMC layer was significantly reduced at 173 K and distributed between the grain boundaries from flower-like to strip-like (Fig. 7(c)). Nevertheless, the number of Cu_3Sn on the fracture surface increased slightly at 123 K.

In contrast to the above two solder joints, although the solder with 37 wt.% Pb still mostly fractured in the solder interior, the edge was fractured in the IMC layer with many cracks at 298 K (Fig. 8(a)). As the temperature decreased, the solder joint broke at the interface, but the solder accounted for the majority. At 173 K, a large amount of Cu_6Sn_5 was found at the fracture, and many uniformly distributed substances adhered to the surface of Cu_6Sn_5, which was detected as the Pb phase. When the temperature was lowered to 123 K, the entire cross-section was composed of fine equiaxed Cu_3Sn, which indicated that the solder joints almost failed at the Cu_3Sn layer and there were many tiny cracks distributed between the Cu_3Sn grain boundaries.

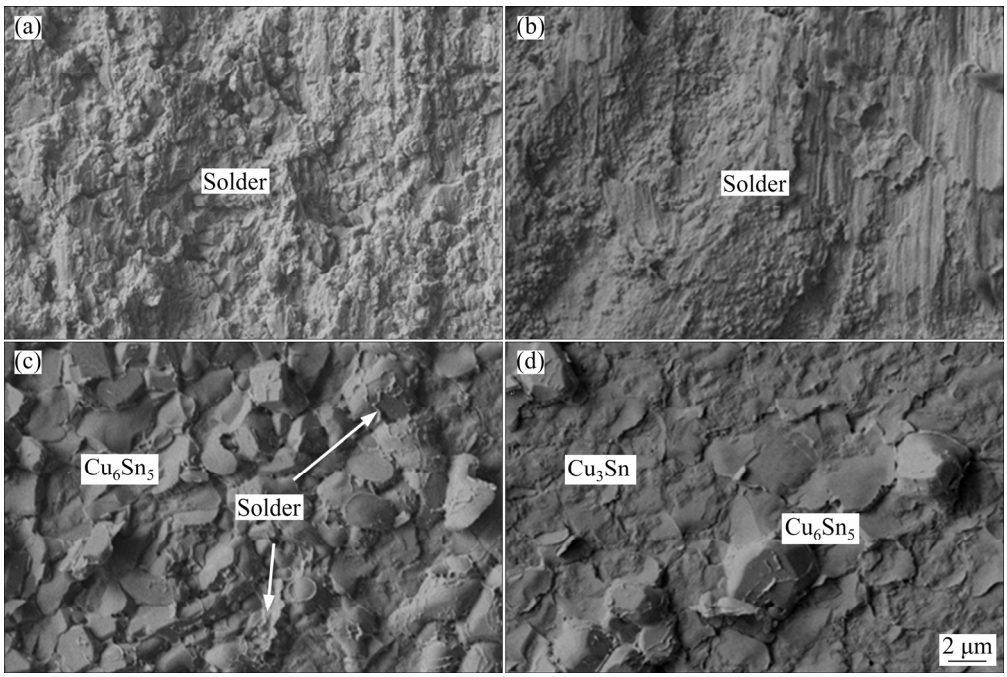

Fig. 7 Fracture surface morphology of mixed solder joints with 22.46 wt.% Pb at different temperatures: (a) 298 K; (b) 223 K; (c) 173 K; (d) 123 K

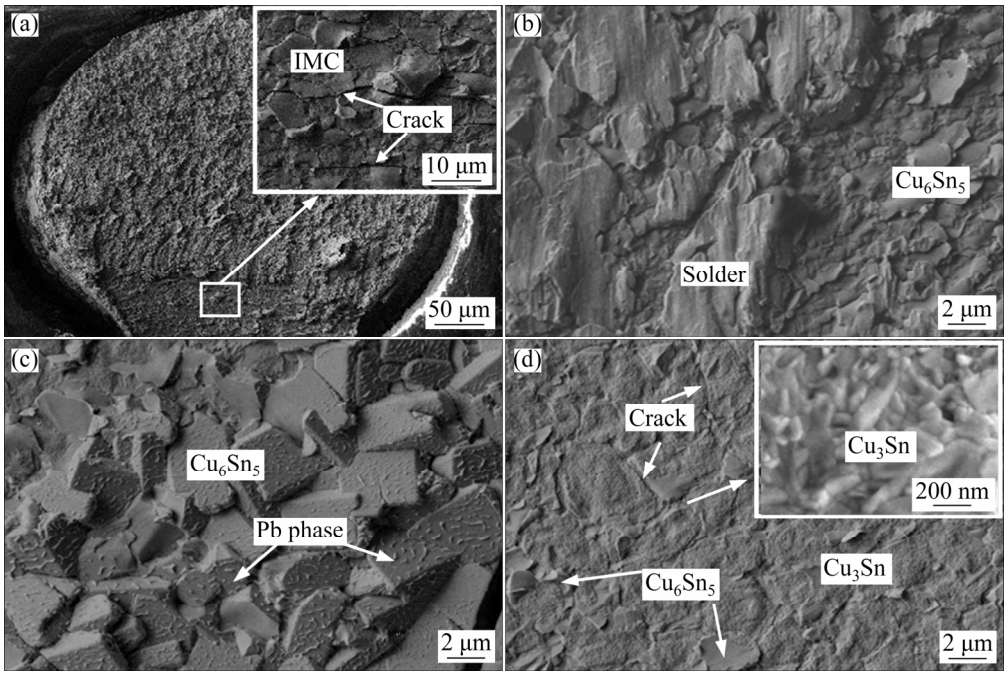

Fig. 8 Fracture surface morphology of solders joints with 37 wt.% Pb at different temperatures: (a) 298 K; (b) 223 K; (c) 173 K; (d) 123 K

4 Discussion

4.1 Mechanical properties

YAZZIE et al [15,19] reported that at low tensile rates, the fracture mode of the solder joint is determined mainly by the solder, and the fracture mode has a great relationship with the slip phenomenon inside the material. Under the action of tensile stress, the elastic deformation of the material crystal occurs first. Beyond this category, due to the increase in the tensile force, the relative displacement between Sn grains produces significant plastic deformation. In addition, the decrease in temperature suppresses the occurrence of sliding, resulting in a continuous decrease in plastic deformation. Finally, brittle fracture occurred at 123 K. It is well known that cryogenic temperatures will reduce the plasticity of the material, leading to progressive brittle fracture of the welded joint during tension, thus increasing the strength [20]. Combined with the theory of fine-grain strengthening, a smaller grain boundary area is beneficial to enhancing the obstacle to grain boundary slippage, resulting in higher strength [21].

For mixed solder joints, the addition of Pb is beneficial to optimizing the mechanical properties of the joint [4]. As a soft phase, Pb easily aggregates at the boundaries of Sn grains and the IMC layer. It helps to release residual stress to enhance the tensile strength during the stretching process. However, the substance is prone to dynamic recovery at normal and high temperatures, and results in reduced flow stress and strength. Conversely, Pb will weaken the thermal activation during dislocations and increase the presence of dislocations, resulting in an increase in the tensile strength at cryogenic temperatures [12,22]. Notably, the addition of excess Pb will separate the Sn grains and accumulate in the IMC layer, especially the 37 wt.% Pb solder joints [23]. This will cause the Pb phase to squeeze with the brittle IMC layer and reduce the performance of the solder joints [24]. Notably, when the Pb content was controlled at 22.46 wt.%, the Pb phase distribution was uniform, which was the reason for the better tensile performance of the 22.46 wt.% Pb joints [4].

4.2 Fracture mode

It is well known that the toughness of materials depends on the electronic type, bonding direction, and degree of symmetry of the structure. The more symmetrical the crystal structure, the more likely the material will undergo ductile fracture [25]. As a multicomponent alloy material, SAC305 solders are mainly composed of β-Sn matrix, and hence, the crystal structure of β-Sn has a considerable influence on the fracture mechanism [26]. The β-Sn has a body-centered tetragonal (bct) structure, and although some studies have shown that β-Sn will transform into a diamond cubic structure α-Sn at cryogenic temperatures. This transformation is very slow and generally has an incubation period of several years. So, β-Sn retains the crystalline form mentioned in Ref. [18].

During the deformation of the metallic material, the diffusion of dislocations leads to an increase in the density of dislocations and in the interaction between dislocations and flow stress. The required performance is the improvement of work hardening [27]. In addition, it is also necessary to overcome the Peierls−Nabarro (P−N) stress (σ_p) that occurs when dislocations pass through the lattice. It is given by the following expression:

$$\sigma_p=\frac{2G}{1-\upsilon}\exp\left(-\frac{4\pi\xi}{b}\right) \tag{1}$$

where G is the tensile modulus of the material, υ is Poisson ratio, ξ is the dislocation half-width, and b is the Burgers vector.

Thus, the dislocation movement is subjected to many resistances such as line tension, long-range interaction force, and applied force during dislocation proliferation. Considering the resistance mechanism of the different dislocations, rheological stress (σ) can be expressed as

$$\sigma=\sigma_p+\alpha\frac{Gb}{l} \tag{2}$$

where α is a coefficient, usually between 0.2−0.5, l is the number of dislocations in the crystals, and the smaller the value of l, the higher the number of dislocations.

From Eqs. (1) and (2), with the decrease in temperature, the P−N stress as well as the rheological stress showed an increasing trend, which leads to an increase in the strength of the solder joints during the tensile process.

According to the Griffith microcrack theory, the small cracks and defects that originally exist in the joint at cryogenic temperatures will exhibit stress concentration phenomena under the action of a tensile stress. Further, due to the difference in the thermal expansion coefficient, the internal cracks in the solder joints continue to expand, which is also the reason for many cracks in Fig. 4(c) [28,29].

For mixed solder joints, because of the difference in the Pb content, the order of phase generation is quite different in solder joints [4,30].

For 4.67 wt.% Pb,

$L \rightarrow L+(Sn)$

$\rightarrow L+(Sn)+\eta-Cu_6Sn_5$

$\rightarrow L+(Sn)+\eta'-Cu_6Sn_5$

$\rightarrow L+(Sn)+\eta'-Cu_6Sn_5+(Pb)$

For 22.46 wt.% Pb,

$L \rightarrow L+(Sn)$

$\rightarrow L+(Sn)+\eta-Cu_6Sn_5$

$\rightarrow L+(Sn)+\eta'-Cu_6Sn_5+(Pb)$

For 37 wt.% Pb,

$L \rightarrow L+(Sn)$

$\rightarrow L+(Sn)+\eta'-Cu_6Sn_5+(Pb)$

From the above, it can be known that the increase in Pb content will change the order of precipitation of the compound and accelerates the precipitation of the Cu_6Sn_5 and Pb phases.

According to the Sn−Pb binary phase diagram, when the Pb content exceeds 22.46 wt.%, a large quantity of the Pb phase begins to deposit near the IMC layer. It becomes an insulating layer between Sn in the solder and Cu in the Cu substrate, slowing the reaction.

At the same time, the interface reaction between Cu_6Sn_5 and the Cu substrate occurs as $Cu_6Sn_5 \rightarrow Cu_3Sn$. Compared with the formation of Cu_6Sn_5, the growth of Cu_3Sn would further reduce the free energy of the system and tend to favor the generation of Cu_3Sn in kinetics. This reaction is intensified as the temperature decreases, causing the 37 wt.% Pb solder joints to break to Cu_3Sn at 123 K [4,31].

During the stretching process, the edge is prone to stress concentration due to its own weakness and the CET mismatch of the components in the solder joints [1,32]. Especially when there is a certain thickness of IMC in the solder joints, cracks will appear along or outside the IMC layer. Due to the lowed solder distribution at the edge and the brittleness of the IMC layer itself, cracks are easy to initiate and expand in these places, resulting in the situation of Fig. 8(a) [33].

At present, most scholars agree with concept of three basic failure modes [3−14]. Through experiments on solder joints, this study also confirmed that the cryogenic temperature and Pb content influenced the transformation of the fracture mechanism of solder joints from the initial ductile fracture to the ductile−brittle mixed fracture and finally to the brittle fracture. However, the mixed fracture mode is more complex, and LAMBRINOU et al [18] and DU et al [34] subdivided the mixed fracture mode into the quasi-ductile fracture (more than 50% fracture in solder) and quasi-brittle fracture (more than 50% fracture in IMC layer). Along with the results of this study, the fracture mechanism is classified as Fig. 9.

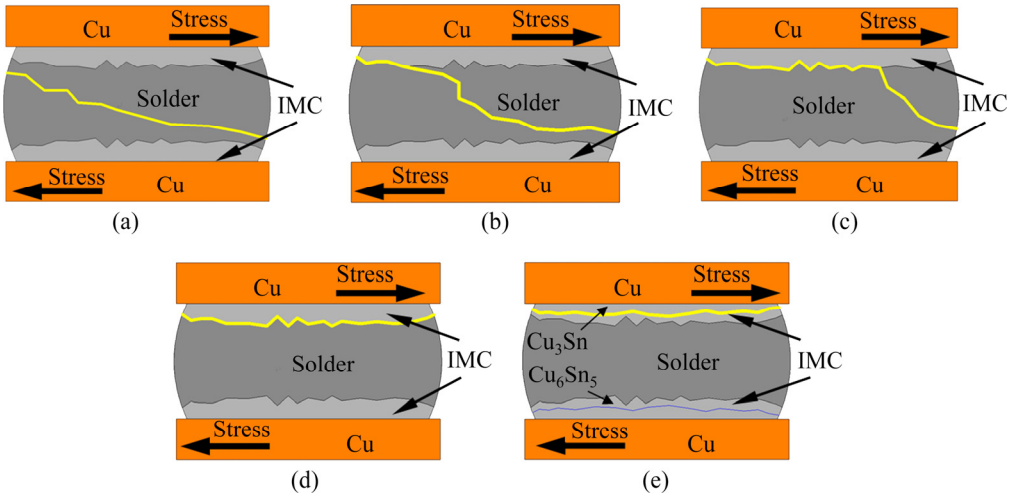

Fig. 9 Transition of fracture mechanism of solder joints: (a) Ductile fracture; (b) Quasi-ductile fracture; (c) Quasi-brittle fracture; (d) Brittle fracture of Cu_6Sn_5; (e) Brittle fracture of Cu_3Sn

Figure 10 shows the transition of the fracture mode of solder joints owing to the temperature and Pb content, and the letter in the figure corresponds to the fracture mode in Fig. 9. At 298 K, the increase in Pb content leads the solder joints to transition from ductile fracture (Fig. 9(a)) to quasi-ductile fracture (Fig. 9(b)). At cryogenic temperature, the Pb content also promoted the transition of the fracture mode, but the variation interval is limited. On the contrary, as the temperature decreases, the fracture position of the solder joints moved continuously from the interior of the solder to the interface, gradually transforming to quasi-ductile fracture (Fig. 9(b)) and quasi-brittle fracture (Fig. 9(c)), and eventually, brittle fracture occurred at 123 K. In particular, the solder joint with 37 wt.% Pb is broken at the Cu_3Sn layer of IMC at 123 K (Fig. 9(e)), which indicates that the decrease in temperature influences the transition of the fracture mechanism of the solder joint.

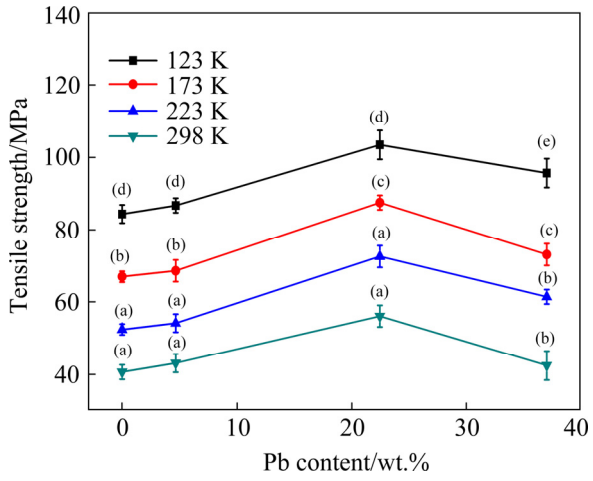

Fig. 10 Fracture mode of solder joints at different Pb contents and temperatures, corresponding to fracture mode in Fig. 9

5 Conclusions

(1) Cryogenic temperature and Pb content have a considerable influence on the tensile strength of mixed solder joints. The increase in Pb content can improve the tensile strength. When the Pb content is 22.46 wt.%, the best effect is achieved, and then, it gradually decreases with the increase in Pb content.

(2) Pb content and cryogenic temperature will lead to change in the fracture mode of mixed solder joints, but the temperature is the dominant factor. The decrease in temperature causes the solder joint to change its failure mode from ductile to quasi-ductile and then, to quasi-brittle fracture, until finally, the brittle fracture mode is attained.

Acknowledgments

The authors are grateful for the financial supports from the National Natural Science Foundation of China (No.51965044), and the Aeronautical Science Foundation of China (No. 20185456005).

References

[1] TUNTHAWIROON P, KANLAYASIRI K. Effects of Ag contents in Sn−*x*Ag lead-free solders on microstructure, corrosion behavior and interfacial reaction with Cu substrate [J]. Transactions of Nonferrous Metals Society of China, 2019, 29(8): 1696−1704.

[2] FAZAL M A, LIYANA N K, RUBAIEE S, ANAS A. A critical review on performance, microstructure and corrosion resistance of Pb-free solders [J]. Measurement, 2018, 134: 897−907.

[3] TAN Shi-hai, HAN Jing, GUO Fu. Recrystallization behavior in mixed solder joints of BGA components during thermal shock [J]. Journal of Electronic Materials, 2018, 47(7): 4156−4164.

[4] WANG F J, O'KEEFE M, BRINKMEYER B. Microstructural evolution and tensile properties of Sn−Ag−Cu mixed with Sn−Pb solder alloys [J]. Journal of Alloys and Compounds, 2009, 477(1−2): 267−273.

[5] TIAN Ru-yu, HANG Chun-jin, TIAN Yan-hong, ZHAO Li-you. Growth behavior of intermetallic compounds and early formation of cracks in Sn−3Ag−0.5Cu solder joints under extreme temperature thermal shock [J]. Materials Science and Engineering A, 2018, 709: 125−133.

[6] TIAN Ru-yu, TIAN Yan-hong, WANG Chen-xi, ZHAO Li-you. Mechanical properties and fracture mechanisms of Sn−3.0Ag−0.5Cu solder alloys and joints at cryogenic temperatures [J]. Materials Science and Engineering A, 2017, 684: 697−705.

[7] PHUA E J R, LIU M, CHO B, LIU Q, AMINI S, HU X, GAN C L. Novel high temperature polymeric encapsulation material for extreme environment electronics packaging [J]. Materials & Design, 2018(141): 202−209.

[8] KANLAYASIRI K, KONGCHAYASUKAWAT R. Property alterations of Sn−0.6Cu−0.05Ni−Ge lead-free solder by Ag, Bi, in and Sb addition [J]. Transactions of Nonferrous Metals Society of China, 2018, 28(6): 1166−1175.

[9] ZHANG Xiang-zhao, WU Xiao-lang, LIU Gui-wu, LUO Wen-qiang, GUO Ya-jie, SHAO Hai-cheng, QIAO Gun-jun. Wetting of molten Sn−3.5Ag−0.5Cu on Ni−P(−SiC) coatings deposited on high volume faction SiC/Al composite [J]. Transactions of Nonferrous Metals Society of China, 2018,

28(9): 1784−1792.

[10] AN Tong, QIN Fei. Effects of the intermetallic compound microstructure on the tensile behavior of Sn3.0Ag0.5Cu/Cu solder joint under various strain rates [J]. Microelectronics & Reliability, 2014, 54(5): 932−938.

[11] ZENG G, MCDONALD S D, MU D K, TERADE Y, YASUDE H, GU Q F, SALLEH M M, NOGITA K. The influence of ageing on the stabilisation of interfacial (Cu, $Ni)_6(Sn, Zn)_5$ and (Cu, Au, $Ni)_6Sn_5$ intermetallics in Pb-free Ball Grid Array (BGA) solder joints [J]. Journal of Alloys and Compounds, 2016, 685: 471−482.

[12] MOLNAR A, JANOVSZKY D, KARDOS I, MOLNAR I, GACSI Z. Effect of Ag and Pb addition on microstructural and mechanical properties of SAC 105 solders [J]. Journal of Electronic Materials, 2015, 44(10): 3863−3871.

[13] FINK M, FABING T, SCHEERER M, SEMERADA E, DUNN B. Measurement of mechanical properties of electronic materials at temperatures down to 4.2 K [J]. Cryogenics, 2008, 48(11): 497−510.

[14] YAO Yao, LI Xiao, HE Xu. Effect of deep cryogenic treatment on mechanical properties and microstructure of Sn3.0Ag0.5Cu solder [J]. Journal of Materials Science: Materials in Electronics, 2018, 29(6): 4517−4525.

[15] YAZZIE K E, FEI H E, JIANG H, CHAWLA N. Rate-dependent behavior of Sn alloy−Cu couples: Effects of microstructure and composition on mechanical shock resistance [J]. Acta Materialia, 2012, 60(10): 4336−4348.

[16] ZHU Yong-xin, LI Xiao-yan, GAO Rui-ting, WANG Chao. Effect of hold time on the mechanical fatigue failure behavior of lead-free solder joint under high temperature [J]. Journal of Materials Science: Materials in Electronics, 2014, 25(9): 3863−3869.

[17] YANG C R, LE F L, LEE S W R. Experimental investigation of the failure mechanism of Cu–Sn intermetallic compounds in SAC solder joints [J]. Microelectronics Reliability, 2016, 62: 130−140.

[18] LAMBRINOU K, MAURISSEN W, LIMAYE P, VANDEVELDE B, VERLINDEN B, WOLF I D. A novel mechanism of embrittlement affecting the impact reliability of tin-based lead-free solder joints [J]. Journal of Electronic Materials, 2009, 38(9): 1881−1895.

[19] YAZZIE K E, XIE H X, WILLIAMS J J, CHAWLA N. On the relationship between solder-controlled and intermetallic compound (IMC)-controlled fracture in Sn-based solder joints [J]. Scripta Materialia, 2012, 66(8): 586−589.

[20] EID E A, FOUDA A N, DURAIA E S M. Effect of adding 0.5 wt.% ZnO nanoparticles, temperature and strain rate on tensile properties of Sn−5.0wt.%Sb–0.5wt.%Cu (SSC505) lead free solder alloy [J]. Materials Science and Engineering A, 2016, 657: 104−114.

[21] EL-DALY A A, FAWZY A, MOHAMAD A Z, EL-TAHER A M. Microstructural evolution and tensile properties of Sn–5Sb solder alloy containing small amount of Ag and Cu [J]. Journal of Alloys and Compounds, 2011, 509(13): 4574−4582.

[22] WANG Xin, LI Xun-ping, ZHOU Bin, JIANG Ting-bao. Effect of Pb content on shear performance of SnAgCu−*x*SnPb/Cu mixed solder joint [C]//2014 15th International Conference on Electronic Packaging Technology. IEEE, 2014: 1173−1176.

[23] TIAN Ru-yu, HANG Chun-jin, TIAN Yan-hong, XU Ji-kai. Brittle fracture of Sn−37Pb solder joints induced by enhanced intermetallic compound growth under extreme temperature changes [J]. Journal of Materials Processing Technology, 2019, 268: 1−9.

[24] WEN Qiang, LI Xun-ping, LI Guo-yuan. Effect of Pb content on thermal fatigue life of mixed SnAgCu−SnPb solder joints [C]//2016 17th International Conference on Electronic Packaging Technology. IEEE, 2016: 1369−1372.

[25] PRASAD R. Surface mount technology: Principles and practice [M]. Springer Science & Business Media, 2013.

[26] TERASHIMA S, KARIYA Y, HOSOI T, TANAKA M. Effect of silver content on thermal fatigue life of Sn−*x*Ag−0.5Cu flip-chip interconnects [J]. Journal of Electronic Materials, 2003, 32(12): 1527−1533.

[27] HE Xu, YAO Yao. A dislocation density based viscoplastic constitutive model for lead free solder under drop impact [J]. International Journal of Solids and Structures, 2017, 120: 236−244.

[28] BAGRETS N, BARTH C, WEISS K P. Low temperature thermal and thermo-mechanical properties of soft solders for superconducting applications [J]. IEEE Transactions on Applied Superconductivity, 2013, 24(3): 1−3.

[29] ZHOU Wei, LIU Li-juan, WU Ping. Structural, electronic and thermo-elastic properties of Cu6Sn5 and Cu5Zn8 intermetallic compounds: First-principles investigation [J]. Intermetallics, 2010, 18(5): 922−928.

[30] LI Xun-ping, ZHOU Bin, WEI Xiong-feng, EN Yun-fei, WANG Xin. The effect of Pb content on the solidification behavior and shear performance of Sn3.0Ag0.5Cu/Cu joint [C]//2014 10th International Conference on Reliability, Maintainability and Safety (ICRMS). IEEE, 2014: 215−219.

[31] DAVIS J A, BOZACK M J, EVANS J L. Effect of (Au, Ni)Sn4 evolution on Sn−37Pb/ENIG solder joint reliability under isothermal and temperature-cycled conditions [J]. IEEE Transactions on Components and Packaging Technologies, 2007, 30(1): 32−41.

[32] TIAN Ru-yu, HANG Chun-jin, TIAN Yan-hong, FENG Jia-yun. Brittle fracture induced by phase transformation of Ni−Cu−Sn intermetallic compounds in Sn−3Ag−0.5Cu/Ni solder joints under extreme temperature environment [J]. Journal of Alloys and Compounds, 2019, 777: 463−471.

[33] TIAN Y, LIU X, CHOW J, WU Y P, SITARAMAN S K. Experimental evaluation of SnAgCu solder joint reliability in 100 μm pitch flip-chip assemblies [J]. Microelectronics Reliability, 2014, 54(5): 939−944.

[34] DU Xue, TIAN Yan-hong, ZHAO Xin. Mechanical properties and microstructure of Sn-based solder joints at cryogenic temperature [C]//International Conference on Electronic Packaging Technology. IEEE, 2014: 888−892.

低温下 SnAgCu−SnPb 混装焊点断裂模式演变规律

吴 鸣，王善林，孙文君，洪 敏，陈玉华，柯黎明

南昌航空大学 江西省航空构件成形与连接重点实验室，南昌 330036

摘 要：研究低温对 SnAgCu−SnPb 混装焊点力学性能和断裂机理的影响。结果表明，混装焊点的抗拉强度首先随着 Pb 含量的增加而提高，在 Pb 含量为 22.46%(质量分数)时达到最大值，之后随着 Pb 含量的增加而降低，温度的降低会不断增加焊点抗拉强度。Pb 含量以及低温均能导致混装焊点断裂模式的转变，其中低温是主导因素。当温度从 298 K 下降到 123 K，焊点的断裂模式不断由韧性断裂向准韧性、准脆性断裂转变，最终演变为脆性断裂。

关键词：断裂模式；拉伸强度；SnAgCu−SnPb 焊料；低温

(Edited by Xiang-qun LI)